Chinese Chemical Letters 37 (2026) 111863

Contents lists available at ScienceDirect

Chinese Chemical Letters

journal homepage: www.elsevier.com/locate/cclet

Efficient dye-sensitized solar cells based on doubly concerted companion dyes with bulky branched chains on the donors and optimized linkage length

Conglin Liu, Yinglong Li, Yuquan Hu, Qizhao Li, Chengjie Li*, Yongshu Xie*

Key Laboratory for Advanced Materials, Shanghai Key Laboratory of Functional Materials Chemistry, Frontiers Science Center for Materiobiology and Dynamic Chemistry, Institute of Fine Chemicals, School of Chemistry and Molecular Engineering, East China University of Science & Technology, Shanghai 200237, China

ARTICLE INFO

Article history:
Received 28 July 2025
Revised 17 September 2025
Accepted 18 September 2025
Available online 18 September 2025

Keywords:
Dye-sensitized solar cells
Porphyrin
Branched alkyl chains
Concerted companion dyes

ABSTRACT

Based on recently reported high-performance doubly concerted companion (DCC) dye **XW96** constructed by covalently linking a porphyrin dye and an organic dye with hexyl chain protected phenothiazine and fluorenyl indoline donors, respectively, we herein employ a branched 2-ethylhexyl chain to realize better anti-charge-recombination and anti-aggregation abilities, achieving improved photovoltaic behavior. Thus, based on **XW96**, dye **XW98** has been synthesized by introducing branched chains to the donors. As a result, the bulkier donors on both sub-dye units cause spatial repulsion, resulting in more severe twisting, decreased adsorption amount and lowered efficiency, compared to **XW96**. To reduce the steric hindrance, the linker between the two subdye units has been extended on the basis of **XW98** (seven bonds) to give **XW99** (eight bonds) and **XW100** (nine bonds), affording considerably improved adsorption. Notably, **XW99** affords an open-circuit voltage (V_{OC}) of 784 mV, a short-circuit current density (J_{SC}) of 22.08 mA/cm^2, and a high power conversion efficiency (PCE) of 12.54%. Compared with **XW99**, dye **XW100** exhibits a larger percentage of single anchoring despite its larger adsorption amount, leading to a lowered efficiency of 12.25%. This work indicates that combination of bulky branched chains on the donors with optimized linker length is essential for developing efficient DCC sensitizers.

© 2025 Published by Elsevier B.V. on behalf of Chinese Chemical Society and Institute of Materia Medica, Chinese Academy of Medical Sciences.

Since the first report in 1991 [1], dye-sensitized solar cells (DSSCs) have demonstrated broad application prospects owing to their diverse raw material sources, low preparation costs, and ease of fabrication [2]. As an essential component of DSSCs, the dyes are responsible for the generation of excited electrons under irradiation. In this respect, ruthenium complex dyes [3,4], metal-free organic dyes [5,6], and zinc porphyrin dyes [7–14] have been widely employed to fabricate efficient DSSCs. As the analog of chlorophyll in photosynthesis, artificial porphyrins feature tunable optoelectronic properties upon peripheral modification [15,16], emerging as key candidates. However, porphyrin dyes exhibit an absorption valley between the Soret and Q bands, which limits the light-harvesting capability and the power conversion efficiency (PCE). Hence, intermolecular cosensitization of porphyrins with spectrally complementary organic dyes has been carried out to achieve panchromatic absorption and high PCEs [17]. For this approach, the dye adsorption faces challenging optimization process, since the soaking sequence and competitive adsorption need to be taken into consideration among other factors [18–21]. To address this issue, concerted companion (CC) dyes [22–29] has been developed, in which intramolecular co-sensitization is achieved by covalently linking a porphyrin sensitizer with an organic sensitizer. Notably, when four C18-alkoxy chains were introduced into the *ortho*-positions of the *meso*–phenyl groups in the porphyrin moiety, the organic dyes were simultaneously protected, and thus doubly concerted companion (DCC) dyes were developed for fabricating DSSCs with high PCE and long-term stability [26]. Thus, DCC dye **XW96** was synthesized by introducing phenothiazine and fluorenyl indoline donors into the porphyrin and organic dye units, respectively (Fig. 1) [29], with multiple hexyl chains attached on the donors to suppress dye aggregation and charge recombination between the oxidized electrolytes and injected electrons and thus improve open-circuit voltage (V_{OC}) [30]. As a result, **XW96** afforded an outstanding PCE of 12.50% [29].

Compared to the long chain substituents on the donors, branched ones have greater steric hindrance, which may provide better protection and thus further suppress charge recombination.

* Corresponding authors.
E-mail addresses: chengjie.li@ecust.edu.cn (C. Li), yshxie@ecust.edu.cn (Y. Xie).

https://doi.org/10.1016/j.cclet.2025.111863
1001-8417/© 2025 Published by Elsevier B.V. on behalf of Chinese Chemical Society and Institute of Materia Medica, Chinese Academy of Medical Sciences.

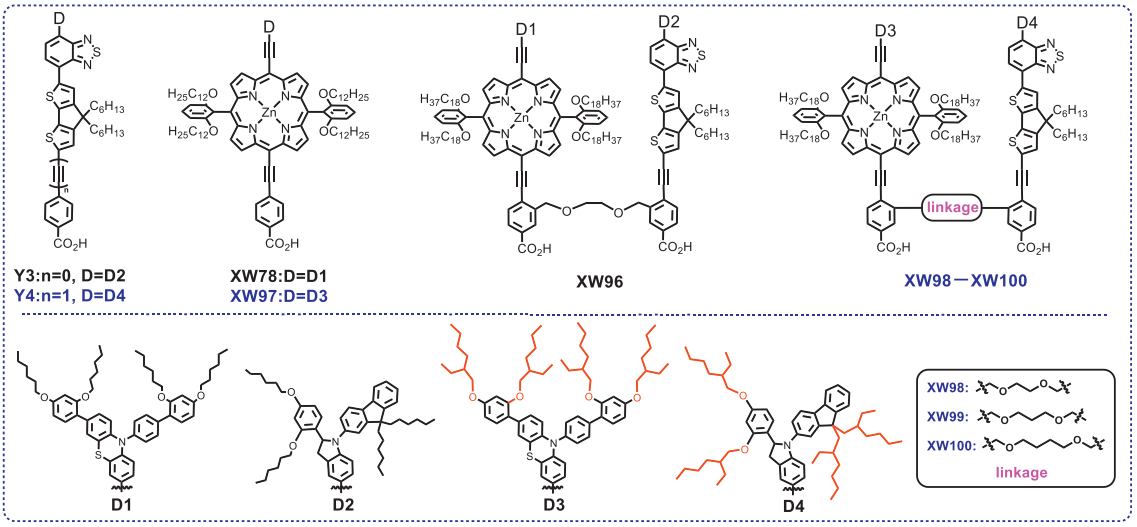


Fig. 1. Molecular structures of organic dyes **Y3** [29], **Y4**, porphyrin dyes **XW78** [26], **XW97**, and DCC dyes **XW96** [29] and **XW98–XW100**.

In this respect, 2-ethylhexyl chain has been shown to be an effective substituent for developing high performance DSSCs [31–33]. Based on this background, we herein report DCC dye **XW98**, which has been synthesized by replacing the hexyl chains on the donors of **XW96** with 2-ethylhexyl chains. Meanwhile, the corresponding organic dye **Y4** and porphyrin dye **XW97** have also been synthesized (Fig. 1). As a result, **XW98** afforded lowered V_{OC} (773 mV), J_{SC} (21.70 mA/cm^2), and PCE (12.13 %), compared to those of **XW96** (782 mV, 21.97 mA/cm^2, and 12.50 %) [29]. Meanwhile, a lowered adsorption amount was observed for **XW98**, probably owing to the severe steric hindrance induced by the bulky donors, which leads to a twisted alignment of the molecule and unsatisfactory anchoring on the TiO_2 film. To release the repulsion, **XW99** and **XW100** have been synthesized by extending the linkage near the anchor from seven single bonds to eight and nine single bonds, respectively (Fig. 1). As expected, the DSSCs based on **XW99** afford higher adsorption amount with elevated V_{OC}, J_{SC} and PCE of 784 mV, 22.08 mA/cm^2, and 12.54 %, respectively. Notably, **XW100** exhibits the highest adsorption amount among these DCC dyes. However, its PCE of 12.25 % is lower than that of **XW99**, which may be related to the larger ratio of single anchoring according to the desorption analysis. These results reveal that judiciously designed bulky donors in combination with optimized linker length is effective for developing efficient DCC sensitizers.

The detailed synthetic routes and procedures for the dyes are outlined in Scheme S1 and described in Supporting information. The structures of all the synthesized compounds were systematically characterized by NMR and mass spectrometry analyses (refer to Supporting information for more details).

The absorption spectra of all the dyes in THF are shown in Fig. 2, with the corresponding data summarized in Table S1 (Supporting information). Obviously, porphyrin dye **XW97** and organic dye **Y4** exhibit complementary absorption profiles. Consequently, the corresponding DCC dyes **XW98**–**XW100** exhibit panchromatic absorption similar to that of **XW96**, indicative of negligible contribution from the alkyl chains on the donors and the linker near the anchors. Upon adsorption of the dyes onto the TiO_2 film, the absorption spectra are significantly broadened (Figs. S1 and S2 in Supporting information), which markedly improves the light-harvesting capability [34]. Notably, the fluorescence spectra of DCC dyes **XW98**–**XW100** are comparable to the addition of the corresponding spectra for the two sub-dyes, indicative of neglectable

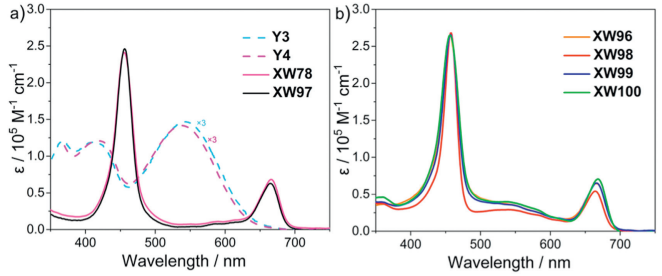


Fig. 2. Absorption spectra of sensitizers. (a) **Y3** [29], **Y4**, **XW78** [26], and **XW97**, and (b) **XW96** [29] and **XW98**–**XW100** in THF.

energy/electron transfer between the porphyrin and organic dye units, which is similar to our previous findings [23,26].

Electrochemical investigations were carried out using cyclic voltammetry (CV) and differential pulse voltammetry (DPV) to determine the redox properties of the sensitizers. As shown in Fig. S4 (Supporting information), the first oxidation potentials (E_{ox}) for **Y4**, **XW97** and **XW98**–**XW100** were found to be 0.75–0.76 V (*vs.* NHE) (Table S2 in Supporting information), considerably lower than that of the I^-/I_3^- redox shuttle (~0.4 V *vs.* NHE), providing sufficient driving forces for dye regeneration. The optical bandgaps (E_{0-0}) were determined *via* the intersection method from normalized absorption and fluorescence emission profiles ($E_{0-0} = 1240/\lambda_{inter}$, Fig. S5 in Supporting information), and thus the lowest unoccupied molecular orbital (LUMO) level values were found to be −1.25, −1.15, −1.23, −1.21, and −1.14 V (*vs.* NHE) for the respective sensitizers, which are obviously higher that of the conduction band of TiO_2 (−0.5 V *vs.* NHE), thermodynamically favorable for electron injection into TiO_2 [35,36].

On this basis, the photovoltaic performance was evaluated under simulated sunlight (AM 1.5 G, 100 mW/cm^2), using I^-/I_3^- as the electrolyte (Figs. 3a and b), and the photovoltaic parameters are summarized in Table 1. As a result, the organic dye **Y4** affords slightly higher V_{OC} (755 mV) with respect to that of **Y3** (747 mV), demonstrating the superiority of the 2-ethylhexyl chains in suppressing charge recombination. However, the bulky donor moiety of **Y4** leads to reduced dye loading (**Y4** = 1.53×10^{-7} mol/cm^2, **Y3** = 1.77×10^{-7} mol/cm^2), resulting in lowered J_{SC} (19.05 mA/cm^2) compared to **Y3** (19.24 mA/cm^2). Because of this trade-off effect, very close PCE values were obtained for **Y4** (10.28 %) and **Y3**

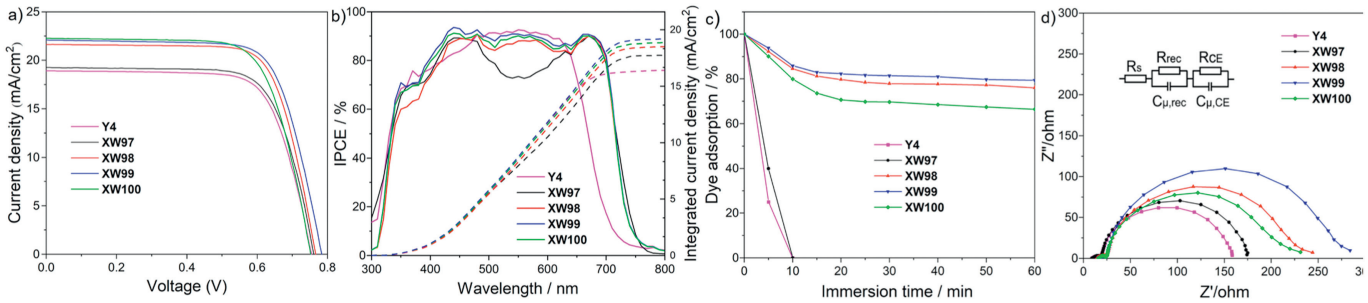


Fig. 3. (a) *J–V* curves, (b) IPCE spectra and integral J_{SC} curves for the DSSCs based on **Y4** and **XW98–XW100** using iodine-based electrolytes. (c) Plots of the decrease in dye adsorption amounts *versus* the immersion time in 0.01 mol/L NaOH solution (THF/H_2O, 1/1), and (d) complex-plane plots at an applied voltage of −0.75 V of the DSSCs based on the investigated dyes.

Table 1
Photovoltaic parameters of the DSSCs based on the dyes under simulated AM 1.5 G sunlight illumination.[a]

Dyes	V_{OC} (mV)	J_{SC} (mA/cm^2)	J_{SC}^{IPCE} (mA/cm^2)[b]	J_{SC} error (%)[c]	fill factor (%)	PCE (%)	Γ (10^{-7} mol/cm^2)
Y3 [29]	747 ± 5	19.24 ± 0.25	16.66	13.4	70.63 ± 0.44	10.20 ± 0.20	1.77
Y4	755 ± 1	19.05 ± 0.13	16.41	13.9	71.53 ± 0.64	10.28 ± 0.05	1.53
XW78 [26]	744 ± 4	19.00 ± 0.17	17.59	7.4	72.54 ± 0.18	10.30 ± 0.10	1.65
XW97	764 ± 3	19.24 ± 0.02	17.73	7.9	71.32 ± 0.80	10.48 ± 0.09	1.67
XW96 [29]	782 ± 2	21.97 ± 0.18	18.60	15.3	72.52 ± 0.42	12.50 ± 0.10	0.93
XW98	773 ± 2	21.70 ± 0.20	18.51	14.3	72.33 ± 0.67	12.13 ± 0.01	0.85
XW99	784 ± 2	22.08 ± 0.12	19.03	13.8	72.44 ± 0.16	12.54 ± 0.12	0.98
XW100	776 ± 2	21.72 ± 0.06	18.75	13.7	72.62 ± 0.26	12.25 ± 0.05	1.05

[a] The data were collected from three parallel cells (average values and errors).
[b] The J_{SC}^{IPCE} values were obtained by integrating the incident photon-to-current conversion efficiency (IPCE) spectra (to further understand the trend for the photocurrents). In general, the IPCE value is determined by the light harvesting efficiency (LHE), charge injection efficiency (η_{inj}), dye regeneration efficiency (η_{reg}) and charge collection efficiency (η_{cc}) (IPCE = LHE (λ) × η_{inj} × η_{reg} × η_{cc}).
[c] The deviations between J_{SC} and J_{SC}^{IPCE}.

(10.20 %) [29]. On the other hand, the presence of branched alkyl chains on the donor of porphyrin dye **XW97** enhances the V_{OC} to 764 mV by 20 mV, compared to reference dye **XW78** [26]. Notably, the bulky donor of **XW97** did not lower the adsorption amount (**XW97** = 1.67×10^{-7} mol/cm^2, **XW78** = 1.65×10^{-7} mol/cm^2). This observation is different from those observed for **Y4** and **Y3**, which may result from the larger size of the porphyrin dye framework with respect to the organic dyes. Thus, the J_{SC} of **XW97** is slightly elevated (19.24 mA/cm^2) compared to **XW78** (19.00 mA/cm^2). As a result, **XW97** exhibits a PCE of 10.48 %, higher than that of 10.30 % obtained for **XW78**. Considering the complementary absorption of **Y4** and **XW97**, they were cosensitized, achieving a PCE of 11.32 % (Table S3 in Supporting information). Compared to the intermolecular co-sensitization method, the panchromatic DCC dye **XW98** affords a considerably enhanced PCE of 12.13 %. However, this efficiency is still lower than that of 12.50 % obtained for **XW96**. This observation may be related to the smaller adsorption amount of **XW98** (0.85×10^{-7} mol/cm^2) with respect to **XW96** (0.93×10^{-7} mol/cm^2), which may result from a twisted arrangement of the two sub-dyes induced by the severe steric hindrance between the bulky donors. The smaller adsorption amount of **XW98** results in lowered light harvesting capability and J_{SC}. In addition, the loosened packing of **XW98** on the TiO_2 surface also leads to aggravated charge recombination and lowered V_{OC}, which is consistent with the electrochemical impedance spectroscopy (EIS) measurements (*vide infra*). To address this issue, the linker near the anchors has been extended from seven to eight single bonds to give **XW99**, achieving an enhanced adsorption amount of 0.98×10^{-7} mol/cm^2. This observation implies that the twisted molecular alignment has been alleviated for **XW99**. As a result, improved V_{OC} (784 mV), J_{SC} (22.08 mA/cm^2), and PCE (12.54 %) have been achieved for the DSSCs based on **XW99**. This efficiency is slightly superior to that of **XW96** (12.50 %). Upon further extending the linkage to nine single bonds (**XW100**), the adsorption amount is further enhanced to 1.05×10^{-7} mol/cm^2. However, the V_{OC} (776 mV) and J_{SC} (21.72 mA/cm^2) are reduced, affording a PCE of 12.25 %, lower than that of **XW99**. Desorption studies reveal a faster desorption process for **XW100**, compared to **XW98** and **XW99** (Fig. 3c), indicative of a higher ratio of single anchoring for **XW100**. To further probe the anchoring behavior of the dyes, ATR-FTIR spectra of the dyes in the powder state and adsorbed on the TiO_2 films have been collected (Fig. S7 in Supporting information). All DCC dyes exhibit a characteristic stretching band of the carboxyl group at *ca.* 1690 cm^{-1}. Upon anchoring onto the TiO_2 films, this peak disappears for **XW98** and **XW99**, while it is only weakened for **XW100**, indicative of nearly complete deprotonation and adsorption of the carboxyl groups for both **XW98** and **XW99**. In contrast, neutral carboxyl group is still present for **XW100** owing to the incomplete anchoring. These results are consistent with the desorption results. Hence, an enhanced adsorption amount is obtained together with a lowered PCE [37]. Based on these results, the DCC dyes were co-adsorbed with CDCA to further improve the photovoltages and efficiencies [38]. Upon coadsorption with 1 mmol/L CDCA, the PCEs of **XW98** and **XW100** could be enhanced to 12.32 % and 12.35 %, respectively. Notably, co-adsorption with 1 mmol/L CDCA did not obviously affect the adsorption amount of **XW98**, indicative of sufficient vacancies on the TiO_2 surface of the **XW98-**based photoanode, which is consistent with the aforementioned hypothesis of the twisted alignment of **XW98** owing to the bulky donors of the two sub-dyes. By contrast, gradual addition of CDCA to **XW99** affords gradually decreased adsorption amounts ($0.93 \times 10^{-7} \sim 0.83 \times 10^{-7}$ mol/cm^2), J_{SC} and PCE (12.39 %~12.13 %) while the V_{OC} remains relatively unchanged. These results indicate that **XW99** possesses remarkable anti-aggregation properties because of the well matched bulky donors and the linker length.

To further understand the photovoltage (V_{OC}) variation trends, electrochemical impedance spectroscopy measurements were carried out. The Nyquist plots feature two semicircles: the smaller left

arcs correspond to the charge transport resistance at the counter electrode/electrolyte interface (R_{tr}), while the larger right arcs represent the recombination resistance (R_{rec}) between oxidized electrolytes and free electrons in the TiO_2 film (Fig. 3d). For the monomeric sensitizers at a fixed bias of 750 mV, the chemical capacitance (C_μ) values were found to be 0.403, 0.321, 0.630, and 0.306 (mF/cm^2) for **Y3**, **Y4**, **XW78**, and **XW97**, respectively (Table S5). Concurrently, the R_{rec} values exhibit increasing trends of **XW78** (46.82 Ω cm^2) < **XW97** (156.3 Ω cm^2) and **Y3** (112.1 Ω cm^2) < **Y4** (140.0 Ω cm^2). As a result, the electron lifetime values ($\tau_{rec} = R_{rec} \times C_\mu$) lie in the increasing order of **XW78** (0.030 s) < **Y3** (0.045 s) = **Y4** (0.045 s) < **XW97** (0.048 s). These results indicate that the 2-ethylhexyl chains can suppress electron recombination more effectively than the hexyl moieties, resulting in longer lifetimes and higher V_{OC}. For the DCC systems, the C_μ values were found to be 0.302, 0.274, 0.253, and 0.262 mF/cm^2 for **XW96**, **XW98**, **XW99**, and **XW100**, respectively, and the R_{rec} values lie in the increasing order of **XW98** (183.4 Ω cm^2) < **XW100** (199.6 Ω cm^2) < **XW96** (200.5 Ω cm^2) < **XW99** (243.0 Ω cm^2). As a result, the electron lifetimes follow the sequence of **XW98** (0.050 s) < **XW100** (0.052 s) < **XW96** (0.061 s) < **XW99** (0.062 s), consistent with the V_{OC} trend. The relatively short electron lifetime and low V_{OC} for **XW98** may be related to the twisted structure induced by the contradiction between the large donors and short linking chain, and the good matching between the bulky donors and the optimized linker length result in the longest electron lifetime and the highest V_{OC} achieved for **XW99** among these DCC dyes (*vide supra*).

To further assess the stability of the DSSCs, long-term irradiation has been performed for 500 h under simulated sunlight conditions. As a result, the PCEs of the monomeric dyes **Y4** and **XW97** are decreased to 82 % and 83 %, respectively, relative to the initial values (Fig. S7 in Supporting information). Under the same conditions, the PCEs of DCC dyes **XW98**, **XW99**, and **XW100** are decreased to 89 %, 91 %, and 89 %, respectively, obviously better than those of the corresponding monomeric dyes, indicative of excellent stability of the DCC dye-sensitized DSSCs is favorable for practical applications.

In summary, a series of DCC dyes have been synthesized by introducing 2-ethylhexyl chains to the donors and optimizing the linker lengths near the acceptors. As a result, the incorporation of 2-ethylhexyl substituents significantly enhance anti-charge recombination capabilities, resulting in improved V_{OC} and PCE for **Y4** (755 mV and 10.28 %) and **XW97** (764 mV and 10.48 %) with respect to the reference dyes **Y3** (747 mV and 10.20 %) and **XW78** (744 mV and 10.30 %), respectively. For the DCC dyes, the large donors and short linker for **XW98** result in detrimental steric hindrance, leading to a twisted molecular alignment, lowered adsorption amount and worsened photovoltaic parameters (J_{SC} = 21.70 mA/cm^2, V_{OC} = 773 mV, FF = 0.7233, PCE = 12.13 %), compared to those of the reference dye **XW96** (J_{SC} = 21.97 mA/cm^2, V_{OC} = 782 mV, FF = 0.7252, PCE = 12.50 %). Relative to **XW98**, the longer linking chain in **XW99** alleviates the steric hindrance, affording improved photovoltaic performance (V_{OC} = 784 mV, J_{SC} = 22.08 mA/cm^2, PCE = 12.54 %), which is the record efficiency for DSSCs based on the I^-/I_3^- electrolyte, to the best of our knowledge. When the linker is further extended, **XW100** exhibits a higher percentage of single anchoring, resulting in decreased V_{OC} (776 mV), J_{SC} (21.72 mA/cm^2) and PCE (12.25 %). In brief, these results indicate that incorporation of bulky branched chains into the donors in combination with well-matched linker length provides an efficient approach for developing efficient DCC sensitizers. Inspired by the results of this work, we are now working on the design of new branched alkyl chains on the donors and linkers between the two subdye units without oxygen atoms for further developing high performance sensitizers.

Declaration of competing interest

The authors declare that they have no known competing financial interests or personal relationships that could have appeared to influence the work reported in this paper.

CRediT authorship contribution statement

Conglin Liu: Writing – original draft, Visualization, Methodology, Investigation, Formal analysis. **Yinglong Li:** Formal analysis, Data curation. **Yuquan Hu:** Formal analysis. **Qizhao Li:** Investigation. **Chengjie Li:** Writing – review & editing, Visualization, Supervision, Methodology, Investigation, Formal analysis, Conceptualization. **Yongshu Xie:** Writing – review & editing, Visualization, Supervision, Methodology, Investigation, Funding acquisition, Formal analysis, Conceptualization.

Acknowledgments

This work at East China University of Science and Technology (ECUST) was financially supported by National Natural Science Foundation of China (Nos. 22131005, 22201074, 22571085), the Fundamental Research Funds for the Central Universities, Shanghai Rising-Star Program (No. 23QA1402100), Shanghai Pujiang Program (No. 24PJD024), Natural Science Foundation of Shanghai (No. 23ZR1415600). The authors thank the Research Center of Analysis and Test of East China University of Science and Technology for compound characterization and thank Professor Yuxin Li from Heilongjiang University for the theoretical calculations.

Supplementary materials

Supplementary material associated with this article can be found, in the online version, at doi:10.1016/j.cclet.2025.111863.

References

[1] B. O'Regan, M. Grätzel, Nature 353 (1991) 737–740.
[2] A.B. Muñoz-García, I. Benesperi, G. Boschloo, et al., Chem. Soc. Rev. 50 (2021) 12450–12550.
[3] A.V. Müller, K.T. de Oliveira, G.J. Meyer, et al., ACS Appl. Mater. Interfaces 11 (2019) 43223–43234.
[4] Y. Xu, L.S. Qiang, Y.L. Yang, et al., Chin. Chem. Lett. 27 (2016) 127–134.
[5] C. Xie, C. Xiao, H. Niu, et al., Chin. Chem. Lett. 35 (2024) 109849.
[6] Q. Bei, B. Zhang, K. Wang, et al., Chin. Chem. Lett. 35 (2024) 108438.
[7] B. Chen, L. Sun, Y.S. Xie, Chin. Chem. Lett. 26 (2015) 899–904.
[8] Y. Lu, H. Song, X. Li, et al., ACS Appl. Mater. Interfaces 11 (2019) 5046–5054.
[9] Y. Tang, Y. Wang, H. Song, et al., Dyes Pigm. 171 (2019) 107776.
[10] K. Zeng, Y. Lu, W. Tang, et al., Chem. Sci. 10 (2019) 2186–2192.
[11] K. Zeng, W. Tang, C. Li, et al., J. Mater. Chem. A 7 (2019) 20854–20860.
[12] Y. Tang, Y. Wang, Q. Yan, et al., Dyes Pigm. 187 (2021) 109075.
[13] Y. Tang, G. Yang, X. Lou, et al., New J. Chem. 45 (2021) 21881–21887.
[14] J. Zou, Y. Tang, G. Baryshnikov, et al., J. Mater. Chem. A 10 (2022) 1320–1328.
[15] N.K. Shee, H.J. Jo, H.J. Kim, Inorg. Chem. Front. 9 (2022) 1270–1280.
[16] Y.H. Zhang, K. Ren, L. Wang, et al., Chin. Chem. Lett. 33 (2022) 33–60.
[17] J.M. Cole, G. Pepe, O.K. Al Bahri, et al., Chem. Rev. 119 (2019) 7279–7327.
[18] Y. Xie, W. Wu, Y. Tang, et al., J. Am. Chem. Soc. 137 (2015) 14055–14058.
[19] P. Roy, A.K. Vats, L. Tang, et al., Sol. Energy 269 (2024) 112339.
[20] Y. Kurumisawa, T. Higashino, S. Nimura, et al., J. Am. Chem. Soc. 141 (2019) 9910–9919.
[21] N.V. Krishna, J.V.S. Krishna, M. Mrinalini, et al., ChemSusChem 10 (2017) 4668–4689.
[22] K. Zeng, Y. Chen, W.H. Zhu, et al., J. Am. Chem. Soc. 142 (2020) 5154–5161.
[23] Y. Chen, Y. Tang, J. Zou, et al., ACS Appl. Mater. Interfaces 13 (2021) 49828–49839.
[24] J. Luo, Z. Xie, J. Zou, et al., Chin. Chem. Lett. 33 (2022) 4313–4316.
[25] X. Wang, Y. Wang, J. Zou, et al., ChemSusChem 15 (2022) e202201116.
[26] J. Zou, Y. Wang, G. Baryshnikov, et al., ACS Appl. Mater. Interfaces 14 (2022) 33274–33284.
[27] J. Luo, Q. Lu, Q. Li, et al., ACS Appl. Mater. Interfaces 15 (2023) 41569–41579.
[28] Y. Wang, Z. Li, Q. Lu, et al., Chin. Chem. Lett. 35 (2024) 109093.
[29] Z. Li, Q. Lu, Y. Zhang, et al., J. Mater. Chem. A 13 (2025) 4176–4185.
[30] M. Grätzel, J. Photochem. Photobiol. C 4 (2003) 145–153.
[31] X.Y. Zhang, Y.Y. Xu, F. Giordano, et al., J. Am. Chem. Soc. 138 (2016) 10742–10745.

[32] E. Tanaka, H. Michaels, M. Freitag, et al., J. Mater. Chem. A 8 (2020) 1279–1287.
[33] M. Jiang, R. Wang, Z.J. Deng, et al., ACS Appl. Mater. Interfaces 16 (2024) 51265–51273.
[34] Y. Wang, B. Chen, W. Wu, et al., Angew. Chem. Int. Ed. 53 (2014) 10779–10783.
[35] K. Zeng, Z. Tong, L. Ma, et al., Energy Environ. Sci. 13 (2020) 1617–1657.
[36] X. Li, P. Song, D. Zhao, et al., Materials 18 (2020) 4834.
[37] J. Luo, Y. Wang, S. Shi, et al., J. Mater. Chem. C 11 (2023) 5450–5460.
[38] K.M. Lee, C.Y. Chen, S.J. Wu, et al., Sol. Energy Mater. Sol. Cells 108 (2013) 70–77.